

Fibre coupled dual-mode waveguide interferometer with $\lambda/130$ fringe spacing

Richard M. Jenkins* and Andrew F. Blockley

Optical Research and Consulting Business Group, QinetiQ, Malvern, Worcs WR14 3PS, U. K.

J. Banerji[†]

Theoretical Physics Division, Physical Research Laboratory, Navrangpura, Ahmedabad 380 009, India

Alan R. Davies[‡]

Dept. of Computer Science, Royal Holloway, University of London, Egham, Surrey TW20 0EX, U.K.

Predictions and measurements of a multimode waveguide interferometer operating in a fibre coupled, “dual-mode” regime are reported. With a $1.32 \mu\text{m}$ source, a complete switching cycle of the output beam is produced by a 10.0 nm incremental change in the $8.0 \mu\text{m}$ width of the hollow planar mirror waveguide. This equates to a fringe spacing of $\sim \lambda/130$. This is an order of magnitude smaller than previously reported results for this form of interferometer.

PACS numbers: 42.25.Bs, 42.25.Hz, 42.79.Gn

The propagation of light through rectangular and planar multimode waveguides can result in interesting self-imaging effects based on multimode interference (MMI) phenomena [1, 2]. Over the last decade or so, these effects have been demonstrated as the basis of splitters [3, 4, 5], modulators and switches [6], Mach-Zehnder interferometers [7] and laser resonators [8].

More recently, Ovchinnikov and Pfau [9] (see also reference [10]) have described a novel form of multimode waveguide interferometer based on a planar waveguide formed from a pair of fully reflecting mirrors. Light enters the planar waveguide at some angle $+\theta$ exciting a spectrum of modes. The ensuing multimode propagation and interference result in oscillations and revivals in the transverse momentum of the propagating field [9]. If L is the length of the multimode guide, λ is the wavelength of the injected radiation, and m is an integer number, then a guide width $w = \sqrt{L\lambda/(4m)}$ maximises the magnitude of the momentum oscillations at the guide exit. Under this condition, small changes in guide width cause the output beam to swing back and forth between the angles of $\pm\theta$.

In their experiment, Ovchinnikov and Pfau [9] coupled a 2.0 mm diameter beam from a $0.633 \mu\text{m}$ source into a 50.0 mm long planar waveguide at an angle of 0.25 radian. With a waveguide width of $30 \mu\text{m}$, a complete cycle of the angular deviation of the output beam was produced by a 70.0 nm change in guide width. The sensitivity to the change in guide width equated to a fringe spacing of $\lambda/9$ [9]. This is substantially smaller than that achieved with a Michelson interferometer.

Although this result is impressive, Ovchinnikov and

Pfau [9] suggested that narrower guide widths ($w \sim \lambda$) should lead to improved sensitivity. They also alluded to the interesting case where only two modes are excited in the planar multimode waveguide, suggesting that the resulting fringe characteristic should be uniform and periodic. If this situation could be realized in practice, then the interferometer could be used over a broader range of contiguous mirror spacings as there would be no “collapse” phenomena to impair operation. Furthermore, with the excitation of only the two lowest order modes, the attenuation in the planar mirror waveguide would be minimized. This is important as, what ultimately limits the sensitivity of this form of interferometer, are the larger attenuation coefficients of the higher order modes.

In this Letter, we show how to implement the proposed dual mode operational regime. Our experimental configuration (see Fig. 1) was similar to that used by Ovchinnikov and Pfau [9]. The planar multimode

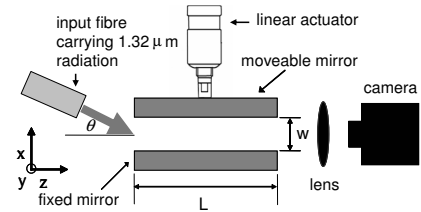


FIG. 1: Schematic of the fibre coupled waveguide interferometer illustrating the input beam and the camera configuration for measuring the near-field output.

waveguide was formed by two 50.0 mm diameter fully reflecting gold coated mirrors both having a surface figure of $\lambda/10$ at 632.8 nm . One of the mirrors was held in a fixed precision mount, the other was mounted on a linear actuator. In our case, $1.32 \mu\text{m}$ radiation from a Nd:YAG laser source was coupled to the planar wave-

*Electronic address: rmjenkins@qinetiq.com

[†]Electronic address: jay@prl.res.in

[‡]Electronic address: alan@cs.rhul.ac.uk

uide from a single-mode, polarization maintaining fibre with an effective $1/e^2$ TEM_{00} mode diameter of $6.5 \mu\text{m}$. The fibre was held straight in a fibre guide and adjusted so that the polarization orientation of the output field was parallel to the plane of the mirror surfaces, i.e. parallel to the y -axis in Fig. 1. Initially the fibre axis was aligned to be co-linear with the planar waveguide axis and butted up to it. Under this condition a choice of $w = 6.5/0.703 = 9.25 \mu\text{m}$, maximizes the power coupling to its fundamental mode [11]. From this starting point, the fibre was tilted by an angle θ with respect to the axis of the planar waveguide. In practice, although the last centimeter of the fibre was stripped back to its $125 \mu\text{m}$ cladding diameter, this still meant that the axis of the fibre pivoted about a $62.5 \mu\text{m}$ radius. Depending on the magnitude of θ , this leads to a short free-space propagation distance and some diffraction before the beam enters the planar waveguide. This was taken into account in the overlap integral calculations to obtain the power coupling coefficients as a function of the input angle θ (see Fig. 2).

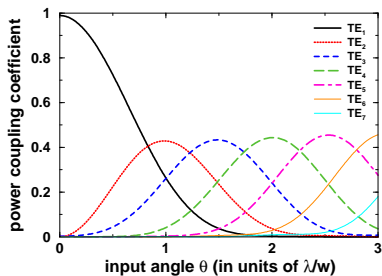


FIG. 2: (color online). Overlap integral calculations illustrating the power coupling coefficients for the modes TE_p as a function of angular misalignment for the case of a TEM_{00} input field.

As θ increases, modes of higher order are excited in turn. The peak in the excitation characteristic of any given higher order mode occurs when the angle of incidence of the input field corresponds to the angle of one of the plane wave components of the higher order mode itself. To a good approximation, to maximize the excitation of the TE_p -th mode, an input beam angle of $\theta = \pm p\lambda/(2w)$ is required. Hence for $p = 2$, one obtains $\theta = \pm\lambda/w = 1.32/9.25 = 0.14$ radian. As indicated in Fig. 2, by choosing an input angle of half this magnitude, i.e. $\lambda/(2w) = 0.07$ radian, the excitation is essentially limited to two modes, TE_1 and TE_2 .

Under this condition, we calculate the sensitivity of the output field to changes in guide width. The phase change between any two TE modes following propagation through an axial distance L , is given by: $\phi_{pq} = L(\beta_p - \beta_q)$

where, β_p is the phase coefficient of the TE_p mode:

$$\beta_p = \frac{2\pi}{\lambda} \left\{ 1 - \left[\frac{p\lambda}{2w} \right]^2 \right\}^{1/2}. \quad (1)$$

Under the condition $(p\lambda/2w)^2 \ll 1$, we get

$$\phi_{pq} = L \frac{\pi\lambda}{4w^2} (q^2 - p^2). \quad (2)$$

Putting $p = 1$ and $q = 2$ for the modes TE_1 and TE_2 respectively, differentiating with respect to the guide width and rearranging, yields:

$$\partial\phi_{12} = -\frac{3L\pi\lambda}{2w^3} \partial w. \quad (3)$$

Equating Eq. 3 to 2π gives the incremental change in guide width that will produce a 2π phase change between the modes, and hence, a change in the output beam angle from $+\lambda/(2w)$ to $-\lambda/(2w)$, and back again, i.e. a fringe, as

$$\partial w = -\frac{4w^3}{3L\lambda}. \quad (4)$$

Eq. 4 leads us to conclude that *small guide widths in conjunction with long waveguides and long wavelength radiation produce maximum sensitivity*. However, reducing the guide width and increasing both the guide length and the wavelength also cause the attenuation of the excited modes to increase in a differential manner. As shown below, this will affect the power ratio between the modes and impact on our ability to measure variations in the output field due to incremental changes in guide width.

The fractional power transmission for the mode TE_p through a planar waveguide of length L is given by

$$t_p = \exp(-2\alpha_p L), \quad \alpha_p = \frac{\lambda^2 p^2}{2w^3} \text{Re}[(\epsilon^2 - 1)^{-1/2}] \quad (5)$$

Here, α_p is the attenuation coefficient and $\epsilon = n - ik$ is the complex refractive index of the wall material. For a $1.32 \mu\text{m}$ source in conjunction with a 50 mm long planar waveguide formed from gold ($n = 0.419$ and $k = 8.42$) coated mirrors, Eq. 5 yields $t_p = \exp(-503p^2/w^3)$. For $w = 7 \mu\text{m}$, this yields fractional transmission values for the modes TE_1 , TE_2 and TE_3 of 0.23, 0.0028 and 1.85×10^{-6} respectively, with $t_1/t_2 \sim 81$. For $w = 11 \mu\text{m}$, the corresponding values are 0.68, 0.22 and 0.03, with $t_1/t_2 \sim 3.1$. From this perspective, with the aim of working with small guide widths in order to achieve high sensitivity, we refer back to Fig. 2 and opt for an input angle of $\pm\lambda/w$. This provides the highest starting magnitude of TE_2 , while the additional excitation of the modes TE_3 and TE_4 are of little consequence because of their significantly higher attenuation.

On the aforementioned basis, we started off with a guide width of $11.0 \mu\text{m}$ with the aim of making measurements of interferometer sensitivity as the width was

decreased to $8 \mu\text{m}$. The launch angle λ/w was kept fixed at 0.14 radian corresponding to a median guide width of $9.25 \mu\text{m}$. To start with, the mirrors were very accurately aligned with respect to one another to ensure that they were parallel. To aid in this process and confirm that dual mode operation was achieved in practice, a magnified (100 times) image of the field generated at the exit of the multimode waveguide interferometer was produced with a microscope objective and viewed with a Hamamatsu infrared vidicon camera C2400-03. The latter has an operational waveband of $0.8 - 2.1 \mu\text{m}$ and a resolution of 720×576 pixels. For a guide width of $11 \mu\text{m}$ and an input angle of 0.14 radian, our predicted transverse intensity profiles at the exit of the planar waveguide are shown in Fig. 3a. These correspond to a $\text{TE}_1:\text{TE}_2$ output power ratio of 1.86 : 1 and phase differences of $-\pi$, $-\pi/2$ and 0 radians induced between these modes by the displacement of the moveable mirror. Fig. 3b shows the results of equivalent measurements made with the camera. The widths of the images correspond to the starting multimode guide width of $11 \mu\text{m}$ while the heights correspond to $100 \mu\text{m}$ high segments of the total vertical extent of the output fields. As a consequence of magnification, the physical dimensions of the images in Fig. 3b are $1.1 \times 10 \text{ mm}$. For presentational purposes, the heights of the images have been compressed by a factor of three. The very good agreement between the measured and predicted field intensity contours confirms that dual mode operation was achieved in practice.

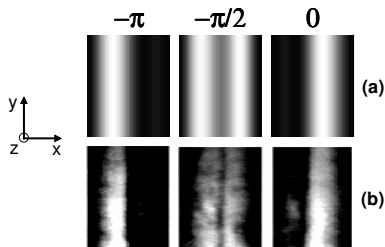


FIG. 3: Near field intensity profiles as a function of the phase difference between the modes TE_1 and TE_2 : (a) predictions; (b) measured profiles.

In order to demonstrate that dual mode operation was achieved over a wide range of contiguous mirror spacings without the presence of the “collapse” phenomena associated with multimode operation, we made a further measurement. This involved accurately locating an InGaAs photo-detector with an effective diameter of 1.0 mm in the plane of the magnified image of the output field. The detector was offset from the axis of the planar multimode waveguide such that its active area only captured light from one side of the image. A linear voltage ramp was then applied in an incremental manner to our New-

port ESA 1330 electro-strictive actuator. At the same time the output from the photo-detector was digitized and recorded. The starting value, and the magnitude of the applied voltage ramp, was chosen to correspond to the most linear portion of the displacement versus applied voltage characteristic of the actuator and to change the planar guide width from an initial value of $11 \mu\text{m}$ to a final value of $8 \mu\text{m}$. The tolerance on the resulting guide width was estimated to be $\pm 0.5 \mu\text{m}$. A plot of the detector output amplitude as a function of the guide width is illustrated in Fig. 4.

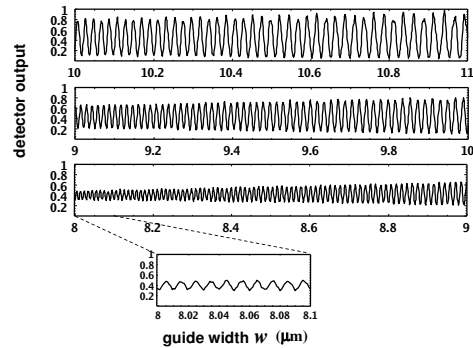


FIG. 4: Experimental measurements of the fringe characteristics as a function of varying guide width w from 11 to $8 \mu\text{m}$. The characteristic illustrates uniformity and periodicity over many cycles with the absence of revival and collapse phenomena in conjunction with decreasing fringe spacing with decreasing guide width. The bottom figure is a higher resolution plot indicating a fringe spacing of $\sim 10 \text{ nm}$ with a guide width of $\sim 8 \mu\text{m}$.

A continuous fringe characteristic is observed. Despite decreasing visibility, it exists over many periods (> 100) and exhibits no collapse phenomena. The bottom figure of the experimental data set illustrates a higher resolution plot indicating a fringe spacing of $\sim 10 \text{ nm}$ with a guide width of $\sim 8 \mu\text{m}$. The decreasing visibility of the fringes with decreasing guide width is a consequence of increased aperturing at the entrance plane, the larger attenuation of both modes, and the higher relative attenuation of the TE_2 mode compared with the fundamental. For values of guide width much below $8.0 \mu\text{m}$ the TE_2 mode amplitude is so small that the fringe visibility becomes comparable with concatenated measurement noise.

In order to more accurately confirm the sensitivity of the interferometer, a further measurement was undertaken. This involved making use of the fringe characteristic itself to calibrate the change in guide width produced by the actuator against a high precision micrometer which was incorporated on the same translational stage. With the actuator calibrated in this manner the applied voltage was changed manually in order to produce ten complete fringe cycles (of the form shown in

Fig. 3b) as observed directly on the vidicon camera with the naked eye. Using this approach, the error in the measurement of the incremental change in guide width necessary to produce a complete switching cycle of the output field was estimated to be of the order of ± 2.0 nm

As illustrated in Fig. 5, these results were plotted as a function of absolute guide width (measured to an estimated accuracy of ± 0.5 μm) together with a theoretical prediction based on Eq. 4. With a guide width of 8.0 μm ,

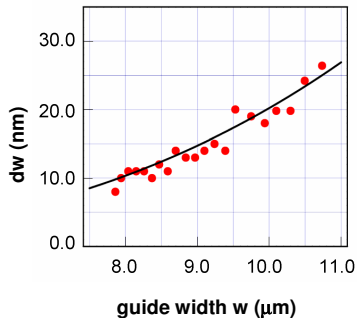


FIG. 5: Experimental measurements (points) and theoretical predictions (solid line based on Eq. 4) of the incremental change in guide width required to produce a complete switching cycle of the near-field output pattern (as illustrated in Figure 3) as a function of guide width.

the measured incremental change in guide width required to produce a complete switching cycle of the output beam was ~ 10.0 nm in agreement with the earlier result. For our 1.32 μm source, this equates to a change in guide width of $\sim \lambda/130$.

In conclusion, an improved multimode waveguide interferometer of the form originally conceived by Ovchinnikov and Pfau [9] has been demonstrated. Our implementation differs from previous work [9] in three main ways: (i) a fibre is used to more efficiently couple the light from the laser source into the planar waveguide, thereby significantly reducing aperturing losses; (ii) the choice of the TEM_{00} waist diameter and the input angle, coupled with the differential attenuation of the excited modes, ensures that only the two lowest order modes (TE_1 and TE_2) are present at the exit plane of the planar waveguide. This leads to the lowest possible attenuation in the waveguide and circumvents the problems of revival and collapse phenomena associated with the excitation of more than two modes [9]. Finally, (iii) the changes in the transverse mode output from the interferometer are measured in the near field. With this implementation a complete cycle of the output field pattern was produced by an incremental change in guide width of ~ 10.0 nm or $\sim \lambda/130$. This should be compared with the $\lambda/9$ change in guide width required to produce a full switching cycle demonstrated in earlier work [9].

A simple analytical expression, given by Eq. 4, has been derived for the sensitivity of the dual-mode interferometer and the way it scales with guide width, guide length and wavelength. Using Eq. 4, predictions of the incremental change in guide width required to produce a complete switching cycle of the output beam are found to be in good agreement with the experimentally measured results as illustrated in Fig. 5.

With respect to achieving higher sensitivity, because of the λ^2 dependence of the attenuation coefficient in Eq. 5, we conclude that it is best to use the shortest operational wavelength possible and, in relation to Eq. 4, to compensate for this by using longer guides and smaller guide widths. Further reduction in attenuation (and hence improved sensitivity) might also be achieved with multilayer mirror coatings designed to provide very high reflectivity for grazing angle incidence TE fields.

We end by noting that dual-mode excitation could also be produced by a laterally offset TEM_{00} beam or by a suitably offset fundamental mode field from an input waveguide. As in the approach described herein, this would result in an output field whose intensity maximum switches from one side of the guide exit to the other. This could be measured with a single or dual-element detector placed directly at the guide exit. This arrangement would make the interferometer more compact facilitating its realisation in silicon based MEMS technology. Thus, multimode waveguide interferometers of the type originally proposed by Ovchinnikov and Pfau [9] should find many sensor and switching applications in the more efficient and more sensitive fibre-coupled dual-mode regime, demonstrated in this paper.

-
- [1] O. Bryngdahl, *J. Opt. Soc. Am.* **63**, 416 (1973).
 - [2] R. Ulrich and G. Ankele, *Appl. Phys. Lett.* **27**, 337 (1975).
 - [3] R. M. Jenkins, R. W. J. Devereux, and J. M. Heaton, *Opt. Lett.* **17**, 991 (1992).
 - [4] J. M. Heaton *et al.*, *Appl. Phys. Lett.* **61**, 1754 (1992).
 - [5] Y B Ovchinnikov, *Opt. Comm.* **182**, 35 (2000); **220**, 229 (2003).
 - [6] R. M. Jenkins, J. M. Heaton and D. R. Wright, *Appl. Phys. Lett.* **64**, 684 (1994).
 - [7] R. M. Jenkins, R. W. J. Devereux, and J. M. Heaton, *Opt. Comm.* **110**, 410 (1994).
 - [8] J. Banerji, R. M. Jenkins, and A. R. Davies, *Appl. Opt.* **36**, 1604 (1997); *J. Opt. Soc. Am.* **14**, 2378 (1997); *Appl. Opt.* **44**, 3364 (2005).
 - [9] Y B Ovchinnikov and T Pfau, *Phys. Rev. Lett.* **87**, 123901 (2001).
 - [10] Y B Ovchinnikov, "A multimode waveguide interferometer", in *Focus on Lasers and Electro-Optics Research*, Ed. W.T. Arkin, pp. 169-185, Nova Science Publishers, New York (2004).
 - [11] D. M. Henderson, *Appl. Opt.* **15**, 1066 (1976)